Supporting Information for "Kinetic-scale current sheets in the solar wind at 5 AU"

I.Y. Vasko[1,2], K. Alimov[3], T.D. Phan[3], F.S. Mozer[3], and A.V. Artemyev[2,4]

[1]William B. Hanson Center for Space Sciences, University of Texas at Dallas, Richardson, TX, USA

[2]Space Research Institute of Russian Academy of Sciences, Russia, Moscow

[3]Space Science Laboratory, University of California, Berkeley, California, USA

[4]Department of Earth, Planetary, and Space Sciences, University of California, Los Angeles, California, USA

Contents of this file

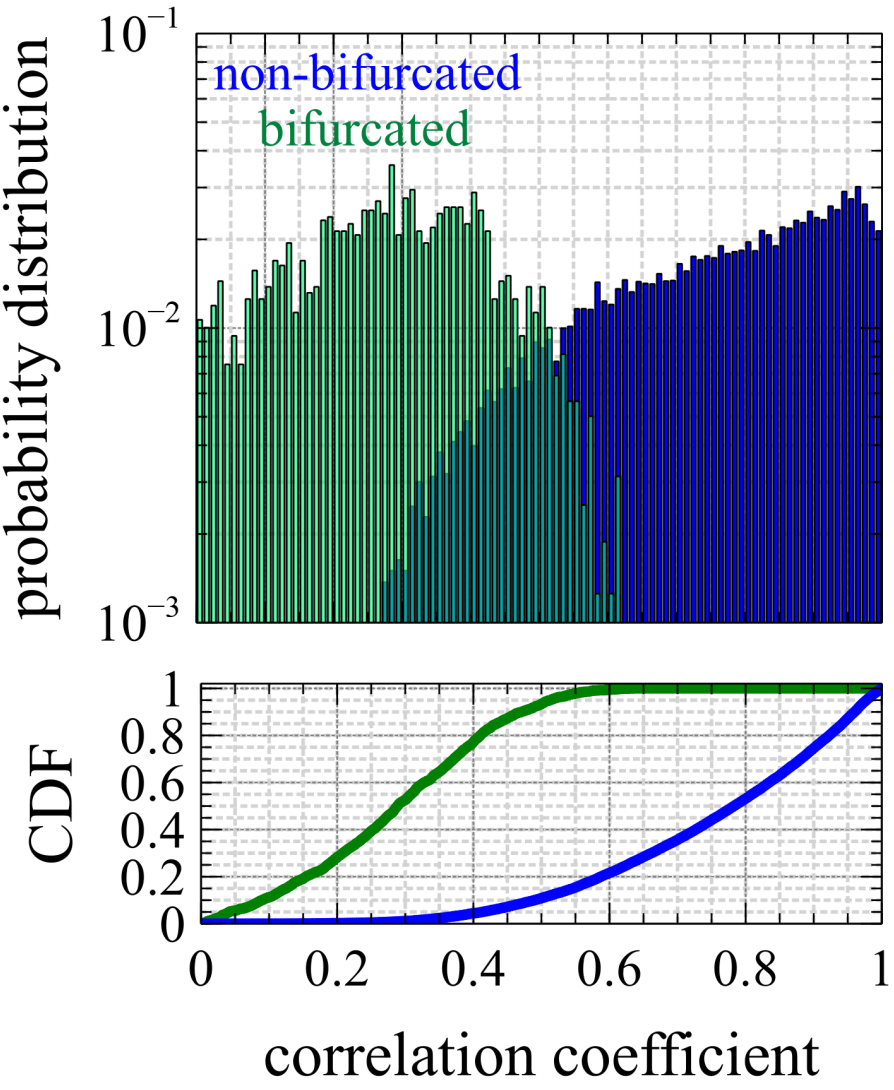

Figure S1. The probability and cumulative distributions of the cross-correlation coefficient between the observed current density profile $J_y(t)$ and a model non-bifurcated profile, $J_{\rm mod}(t) = \langle J_y \rangle \, {\rm sech}^2 \, (t/\tau_{\rm CS})$, where the brackets denote averaging over the CS central region, $t = 0$ corresponds to the middle of the CS central region, and $\tau_{\rm CS}$ is the temporal half-thickness determined by $\Delta B_x/2\tau_{\rm CS} = \langle dB_x/dt \rangle$. The distributions for CSs categorized visually as bifurcated (green) and non-bifurcated (blue) show that the cross-correlation coefficient is below (above) 0.5 for more than 95% (90%) of the bifurcated (non-bifurcated) CSs. This figure substantiates the adequacy of the visual classification of the CSs.

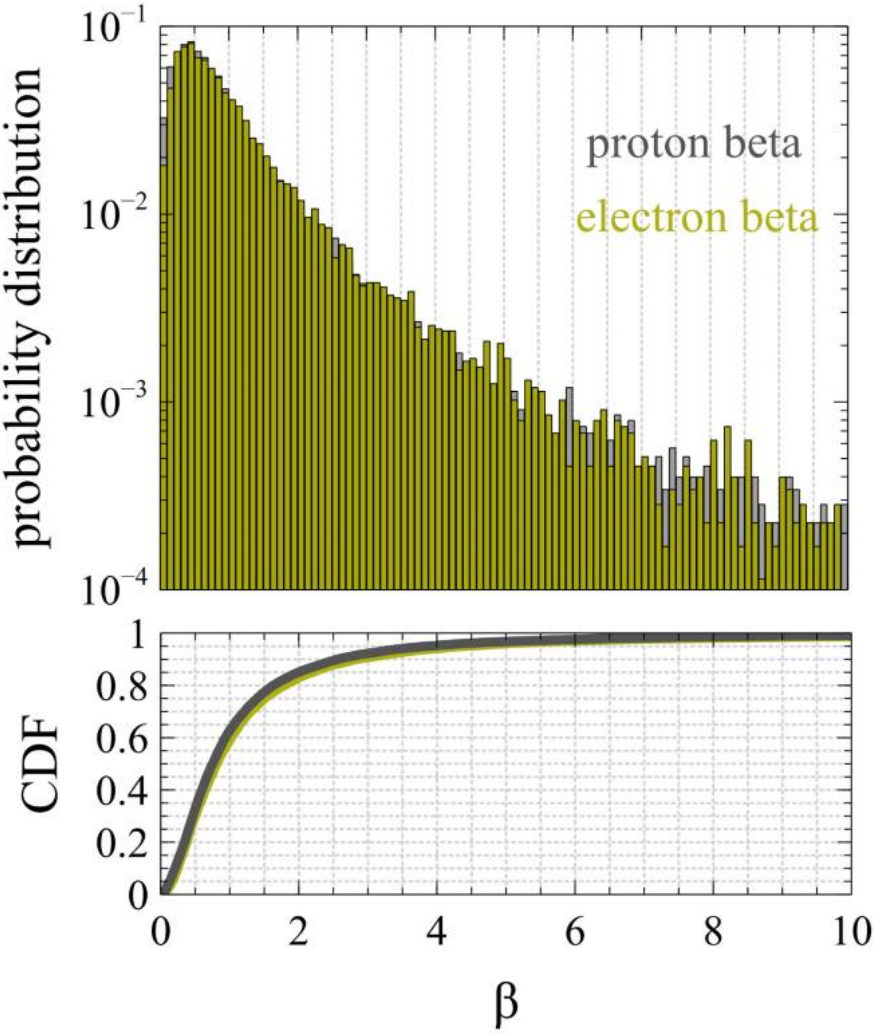

Figure S2. The probability and cumulative distributions of proton and electron betas associated with the CSs in our dataset. This figure supports the statement that in our dataset both electron and proton betas are similar and around one.

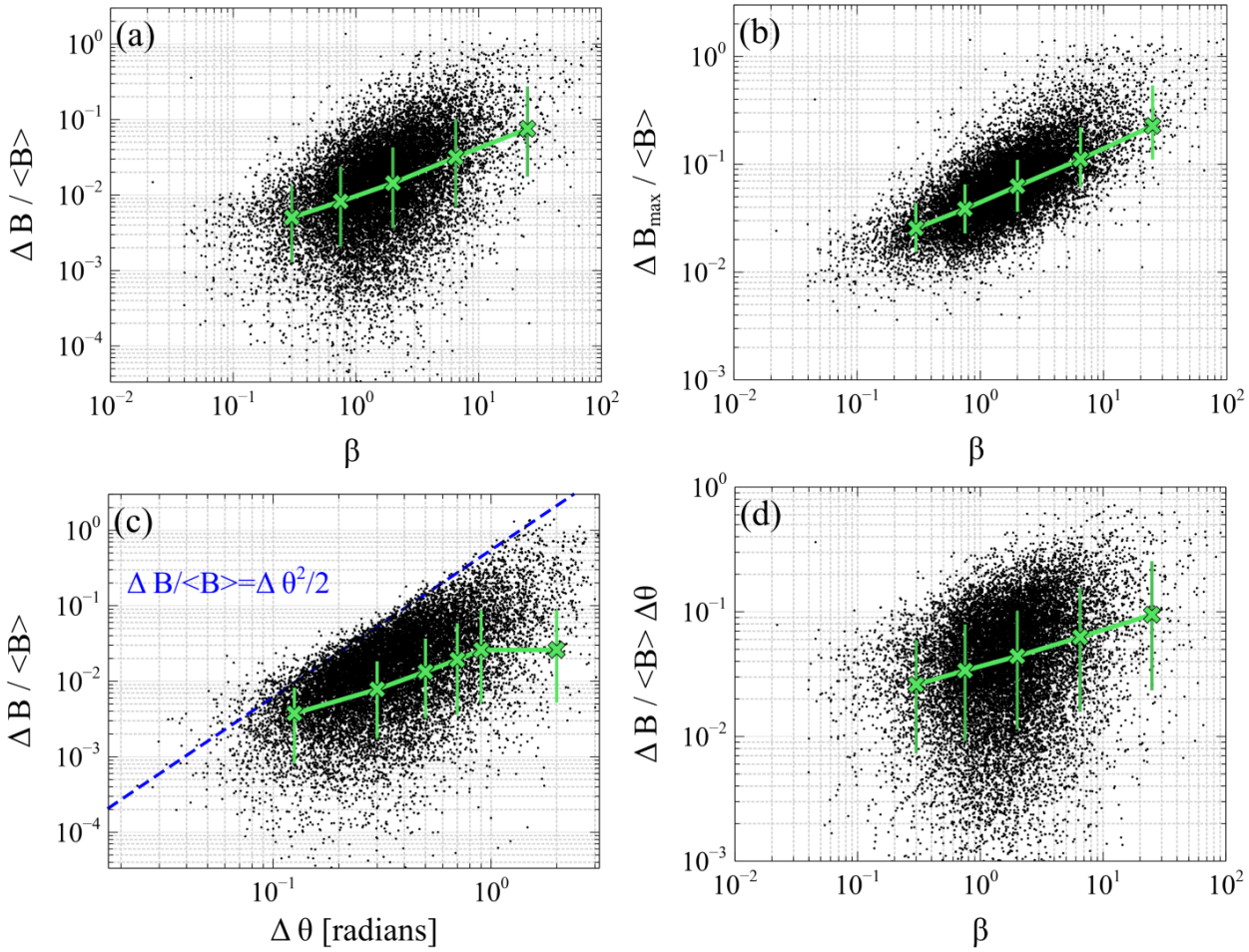

Figure S3. Panels (a), (b) and (d) present scatter plots of plasma beta β versus parameters $\Delta B/\langle B\rangle$, $\Delta B_{\rm max}/\langle B\rangle$ and $\Delta B/\langle B\rangle\Delta\theta$ computed for each CS in our dataset. The latter parameters quantify respectively the relative variation of the magnetic field magnitude between the CS boundaries, the maximum relative variation of the magnetic field magnitude within CS, and the ratio between average perpendicular and parallel current densities within CS. Panel (c) shows the scatter plot of $\Delta B/\langle B\rangle$ versus shear angle $\Delta\theta$. The green curves in all panels were obtained by binning the data and computing the mean value of a quantity of interest within each bin. The error bars reflect the 15th and 85th percentiles within each bin. This figures supports the statement that the relative variations of the magnetic field magnitude and the relative value of the perpendicular current density are not only larger for larger betas, but also positively correlated with plasma beta.

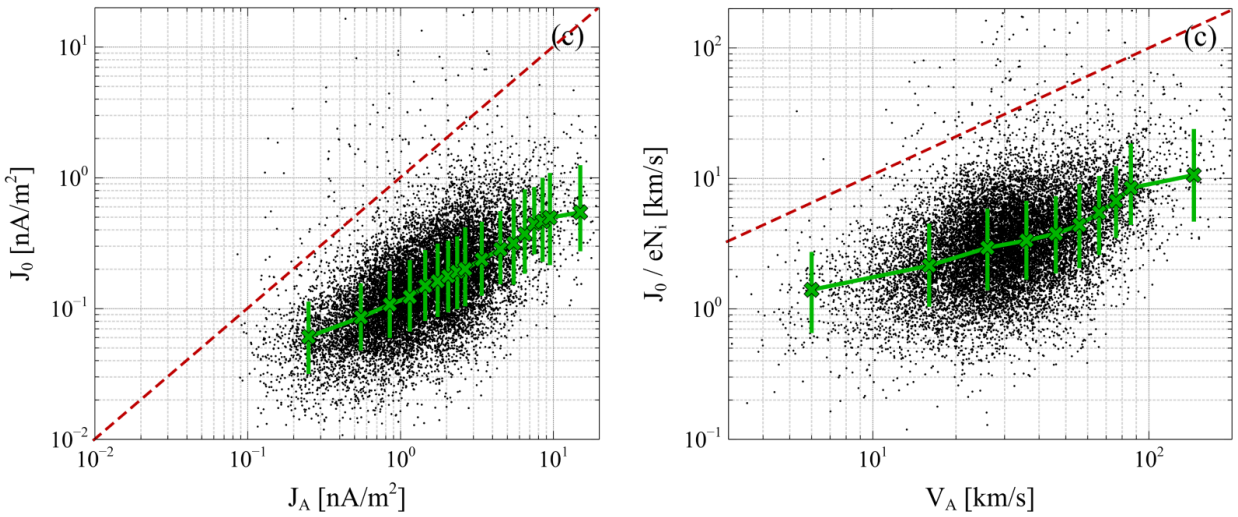

Figure S4. The scatter plots of (a) the averaged current density J_0 versus local Alfvén current density $J_A = eN_iV_A$, where N_i is local plasma density, and (b) the electron-ion drift velocity J_0/eN_i versus local Alfvén speed V_A. The green curves were obtained by binning the data and computing the mean value within each bin. The error bars reflect the 15th and 85th percentiles within each bin. The red lines correspond to the equality of two quantities. This figure supports the statement that the averaged current density J_0 is positively correlated with local Alfvén current density and the corresponding electron-ion drift is positively correlated with local Alfvén speed.

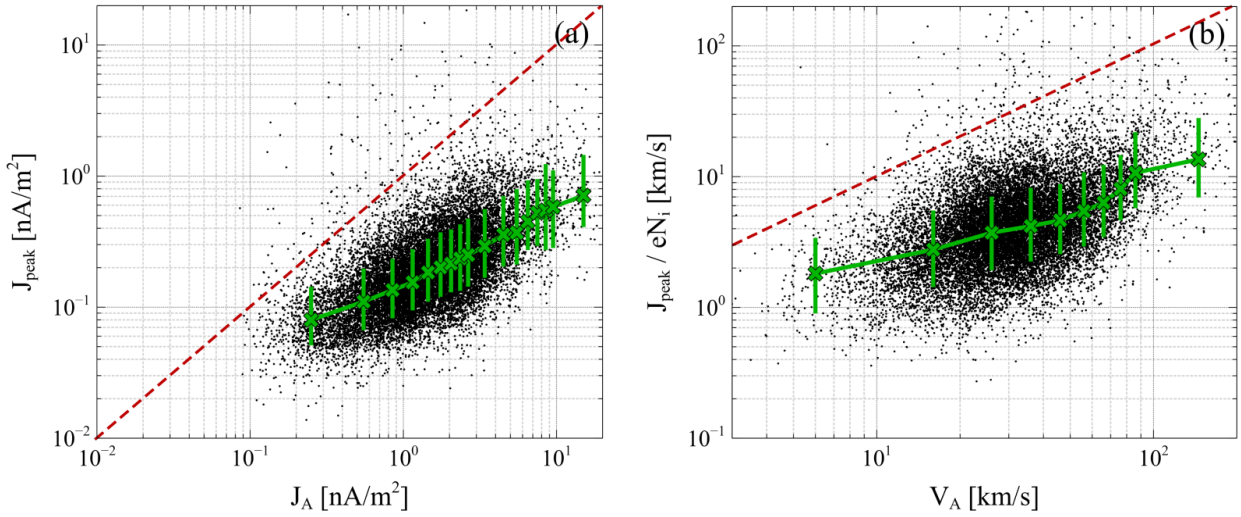

Figure S5. The same as in Figure S4, but for the peak value J_{peak} of the current density. This figure supports the statment that the electron-oion drift corresponding to the peak current density value is positively correlated with local Alfvén speed.